component in cosmic rays. As a first approximation the production of secondary nucleons in high energy nuclear events can be described entirely by methods appropriate to the optical model;[6] the statistical model can be applied as a correction to the nucleons remaining inside the nucleus with excitations of 30 Mev or less.

The present analysis is in harmony with the interpretation of the high energy tail in γ-n excitation curves[7] as largely due to a direct photoelectric effect, especially in light elements. It strongly suggests, however, that this interpretation is not to be applied to the large resonances found in the 17-Mev region among medium and heavy elements, as is already clear from the large peak cross sections.

In case the incident particle to be elastically scattered or absorbed is a π-meson, an important modification is made by the possibility of catastrophic absorption in which the incident particle is destroyed. If this occurs, the nucleus will be excited by more than 140 Mev, and the arguments above indicate that fast nucleon emission will preclude the formation of a compound state. On the other hand, if a compound state is to be formed with the meson as one particle, catastrophic absorption must be avoided for a relatively long time and is the dominant factor determining f. Thus,

$$N_2/N_1 \approx (\tau_2/\tau_1)p^n \approx np^n, \tag{5}$$

where $n \approx \tau_2/\tau_1$ is the number of collisions made by the meson during the establishment of a compound state, and p is the average probability per collision of escaping catastrophic absorption. It appears,[8] at least at moderate energies, that $p \ll 1$; then maximizing (5) shows that $(N_2/N_1)_{\max} \ll 1$, and that this maximum is achieved for $n \ll 2$, which is certainly too few collisions to establish a compound state. Thus one concludes that only the optical model is applicable to calculation of π-mesons on nuclei for all energies. The argument concerning sharp *vs* diffuse boundaries, however, still holds in favor of including nuclear boundary effects in meson calculations.

The author wishes to thank Professor R. Serber for stimulating comments, and Dr. J. M. Miller for an interesting discussion.

[6] M. L. Goldberger, Phys. Rev. **74**, 1269 (1948).
[7] R. Sagane, Phys. Rev. **84**, 587 (1951).
[8] Brueckner, Serber, and Watson, Phys. Rev. **84**, 258 (1951).

PHYSICAL REVIEW VOLUME 86, NUMBER 3 MAY 1, 1952

Extinction Effects in Neutron Transmission of Polycrystalline Media*

R. J. Weiss
Watertown Arsenal, Watertown, Massachusetts
(Received November 29, 1951)

The effects of primary and secondary extinction are considered for neutron transmission work in the energy region where diffraction is important. It is shown that in typical studies the grain size is the most important parameter affecting extinction, with the mosaic block size and the angular spread of the mosaic blocks of secondary importance. Experiments were performed to corroborate the theory, and criteria are set up to avoid extinction effects. It is shown how to determine the mosaic block size and the angular spread of the mosaic blocks in substances with large grain size by using fine resolution near the last crystalline cutoff, where the breadth of the Bragg peak becomes large compared to the angular misalignment of the mosaic blocks.

It is convenient in neutron transmission studies of polycrystalline media to have the apparent cross section per nucleus of the sample, as given by the usual expression $\bar{\sigma} = (\ln I_0/I)/Nx$ (where N is the number of nuclei per cc and x is the thickness of the sample), proportional to the coherent cross section of the nuclei. Previous theoretical treatments[1,2] have assumed this to be the case under the experimental conditions that the microcrystals are randomly oriented and are small enough to give negligible primary extinction. Microcrystals are small coherent domains (commonly called mosaic blocks) and are usually misaligned over a range of several seconds in perfect crystals to several minutes in the macroscopic grains of imperfect crystals like metals. (In large single crystals the gross lineage may cause further misalignment to the extent of several degrees,[3] but we shall confine our attention here to small grains $<10^{-1}$ cm.) It is the purpose of this note to show that the conditions postulated in references 1 and 2 are not sufficient and to point out under what conditions the proportionality between the apparent and coherent nuclear cross sections are assured. We shall also show how it is possible to secure information about the mosaic block size even if primary extinction is negligible.

To begin, we consider the cross section for scattering into Bragg peaks of a perfect microcrystal small enough to make use of the Born approximation,

$$\sigma = \frac{\sigma_{\text{coh}}}{4\pi} \prod_{ijk} \frac{\sin^2(N_i s d\mathbf{q}\cdot\mathbf{i})}{\sin^2(s d\mathbf{q}\cdot\mathbf{i})}, \tag{1}$$

* Research carried out at Brookhaven National Laboratory under contract with AEC.
[1] Halpern, Hamermesh, and Johnson, Phys. Rev. **59**, 981 (1941).
[2] Fermi, Sturm, and Sachs, Phys. Rev. **71**, 589 (1947).
[3] Weiss, Hastings, and Corliss, Phys. Rev. **83**, 863 (1951).

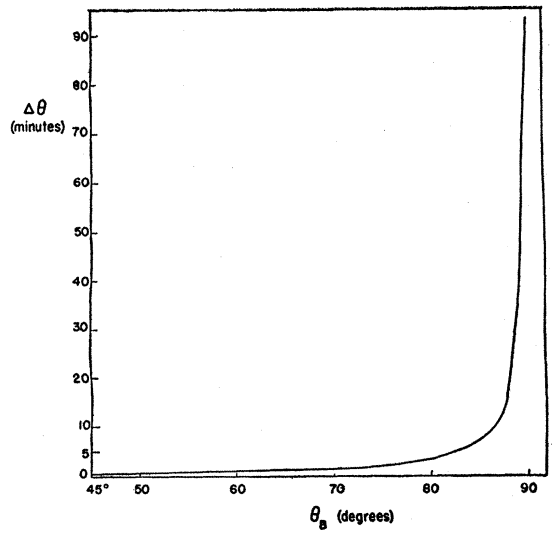

FIG. 1. Half-width in minutes of the 111 Bragg peak in aluminum as a function of Bragg angle for a microcrystal size $t_0=2\times10^{-4}$ cm.

where $\mathbf{q}$ is the unit scattering vector; $\mathbf{i}$, $\mathbf{j}$, $\mathbf{k}$, are unit vectors along the crystallographic axes, N_i is the number of nuclei in the microcrystal in the $\mathbf{i}$ direction, $s=4\pi\sin\theta_B/\lambda$, d=grating space of the diffracting plane, and θ_B is the Bragg angle. When the Bragg conditions are fulfilled, $\mathbf{q}\cdot\mathbf{j}=\mathbf{q}\cdot\mathbf{k}=0$, $\mathbf{q}\cdot\mathbf{i}=1$, $sd=2\pi$, and $\sigma=\sigma_{\text{coh}}N_i^2N_j^2N_k^2=\sigma_{\text{coh}}N^6$. The angle, θ, at which $\sigma=\frac{1}{2}\sigma_{\text{coh}}N^6$ is given by

$$\sin\theta_B-\sin\theta\cong\lambda/2.6t_0, \tag{2}$$

where $t_0=Nd$=size of the microcrystal. When the Bragg angle is not too near the cut-off wavelength, i.e., $\lambda<2d$; $\theta_B<\pi/2$, then (2) becomes

$$\Delta\theta=0.8\lambda/t_0\cos\theta_B. \tag{3}$$

This is the full width at half-maximum of the diffraction peak. When $\theta_B\to\pi/2$

$$\Delta\theta\to(3\lambda/t_0)^{\frac{1}{2}}. \tag{4}$$

This is the full width of the diffraction peak at the cutoff.

For $t_0=2\times10^{-4}$ cm, $\lambda=1$A, and $\theta_B\ll\pi/2$, we find $\Delta\theta\cong15$ seconds, and the assumption in typical differential cross-section studies that microcrystals scatter independently for all but the most perfect crystals appears reasonable. However, for typical transmission studies when $\theta_B\to\pi/2$, and for $t_0=5\times10^{-5}$ cm and $\lambda=4$A, we find $\Delta\theta\cong1.5$ degrees. Since the angle between microcrystals is much less than this, it follows that microcrystals in a grain will either scatter coherently or at least will all satisfy the Bragg conditions simultaneously. Figure 1 is a plot of the half-width as a function of the Bragg angle for the (111) peak in aluminum for a microcrystal size $t_0=2\times10^{-4}$ cm, and it indicates the very rapid rise in half-width as $\theta_B\to\pi/2$. The sharpness of the cutoff, however, is negligibly affected by this large uncertainty in θ_B. To see this we differentiate the Bragg equation and obtain the resolution for the (111) cutoff in aluminum,

$$\frac{\Delta\lambda}{\lambda}=\frac{\Delta\theta}{\tan\theta_B}=\frac{(3\lambda/t_0)^{\frac{1}{2}}}{\tan(\frac{1}{2}\pi-\frac{1}{2}\Delta\theta)}\cong7.8\times10^{-4}, \tag{5}$$

which is much better than the resolution generally obtainable with present instruments.

The effect of this diffraction broadening will be to introduce primary extinction if the grains scatter coherently, or secondary extinction if they do not. When extinction is present, multiple scattering within the crystal redirects a portion of the scattered beam back into the main beam and the exponential decrease in intensity is not observed. It has been pointed out[4] that if the "mosaic block" picture is correct, primary extinction will not be present since the distorted regions between mosaic blocks introduce arbitrary phase differences which destroy the coherence between mosaic blocks. Secondary extinction does become important and, in fact, the experimental evidence below supports this. However, to prove this point a general treatment of both primary and secondary extinction applicable to neutron transmission studies follows. We first consider primary extinction.

PRIMARY EXTINCTION

The integrated reflecting power of a perfect crystal plate of thickness t, i.e., the reflecting power integrated over the angular range of reflections of the crystal is, neglecting temperature effects,[5,6]

$$R^\theta=\frac{\lambda^2NF[|\gamma_H|/|\gamma_0|]^{\frac{1}{2}}}{g\sin2\theta_B}\tanh A, \tag{6}$$

where

$$F=(\sigma_{\text{coh}}/4\pi)^{\frac{1}{2}}\sum_{hkl}\exp[2\pi i(hx/a+ky/b+lz/c)],$$

γ_H and γ_0 are the direction cosines of the diffracted and incident beams with the normal to the surface of the crystal, g is the number of atoms per unit cell, and A, the extinction factor, is given by

$$A=N\lambda Ft/g[|\gamma_H|/|\gamma_0|]^{\frac{1}{2}}. \tag{7}$$

If we introduce the solid angle factor, $(\cos\theta_B)/2$, for randomly oriented crystals in a powder sample and substitute $\sin\theta_B=\lambda/2d$, we have

$$R^\theta=(dN\lambda F/2g)[|\gamma_H|/|\gamma_0|]^{\frac{1}{2}}\tanh A=N\bar\sigma t/\gamma_0\ll1, \tag{8}$$

$$\bar\sigma=(d\lambda F/2gt)[|\gamma_H|/|\gamma_0|]^{\frac{1}{2}}\tanh A. \tag{9}$$

We now distinguish two cases:

Case 1: $A<0.24$, $\tanh A\approx A$, and $\bar\sigma$, the apparent cross section per nucleus is given by

$$\bar\sigma=\lambda^2NF^2d/2g^2. \tag{10}$$

[4] S. Pasternack, private communication.
[5] W. H. Zachariasen, *Theory of X-Ray Diffraction in Crystals* (John Wiley & Sons, Inc., New York, 1945).
[6] G. E. Bacon and R. D. Lowde, Acta Cryst. 1, 303 (1948).

If we introduce the Debye-Waller factor, e^{-2W}, the multiplicity, j, and sum over all planes $\lambda \leq 2d$, we have for typical transmission work

$$\bar{\sigma} = \sum_{\lambda \leq 2d} \frac{\lambda^2 N F^2 j d}{2g^2} e^{-2W} \tag{11}$$

in agreement with former authors.[1,2] The condition, then, to insure negligible primary extinction is,

$$t < 0.24 g \langle [\,|\gamma_0 \gamma_H|\,]^{\frac{1}{2}} \rangle_{Av} / N\lambda F \approx 0.16 g / N\lambda F. \tag{12}$$

Case 2: $10^2 > A > 2$, $\tanh A \to 1$, and

$$\bar{\sigma} = (\lambda dF / \pi g t). \tag{13}$$

$\bar{\sigma}$ is now proportional to $(\sigma_{\text{coh}})^{\frac{1}{2}}$ and inversely proportional to t, making this an inconvenient condition.

In actual grains, if the microcrystals scatter coherently as $\theta_B \to \pi/2$, t becomes an effective thickness (called t^{eff}), which may be large compared to the microcrystal size and less than or equal to the grain size. We shall assume that the microcrystals follow a Gaussian distribution given by

$$W(\epsilon) = \frac{1}{\eta(2\pi)^{\frac{1}{2}}} \exp(-\epsilon^2/2\eta^2), \tag{14}$$

where ϵ is the angle the neutron makes with the mean angle of the blocks and $2(2\ln 2)^{\frac{1}{2}}$ is the half-width. If t^{eff} is proportional to the number of microcrystals in the range $\Delta\epsilon$, then for $\Delta\epsilon \ll \eta$,

$$t^{\text{eff}} \cong T\Delta\epsilon / 2\eta = T\lambda / (2\eta t_0 \cos\theta_B), \tag{15}$$

where T = grain size. Introducing the solid angle factor into (15) and substituting this into (13), we have

$$\bar{\sigma} = (4\eta t_0 dF / \pi g T). \tag{16}$$

$\bar{\sigma}$ is then independent of λ.

If $\Delta\epsilon > \eta$ the entire grain scatters coherently and

$$\bar{\sigma} = (d\lambda F / \pi g \bar{T}), \tag{17}$$

where $\bar{T}$ is an average grain size. Even though the extinction in the grains is complete under these conditions, the angular range over which they reflect is still proportional to λ.

While the sharpness of the cutoff is theoretically limited by (5), it may in practice be limited by the geometry of the detector and sample. The reason for this is that at the cut-off wavelength, the multiply scattered beams are spread out over a small angular range in the forward and backward direction (each scattering deviates the neutron by 180°). The second scattering, even though not in the same grain, may cause the neutron to enter the detector. The use of the exponential law assumes that all scattered neutrons are lost. This effect can be minimized by making the geometry from scatterer to detector less than $(3\lambda/t_0)^{\frac{1}{2}}$ near the cutoff.

It should be noted that Eq. (11) assumes completely random orientation of grains. Preferred orientation is generally present in cold-worked metals and may even be present in annealed metals and compressed powders. To insure the validity of (11) it is suggested that loosely packed powders be used.

SECONDARY EXTINCTION

The integrated reflecting power of a layer of mosaic blocks is given by Zachariasen,[4] Eq. (4.18). We have used Eq. (3.158) for the reflecting power, P_H/P_0, of each mosaic block. This gives for the reflectivity per unit thickness of imperfect crystal

$$\sigma = \frac{A^2}{t_0 \eta \sqrt{2}\,[1/2\eta^2 + A^2 q^2/\pi]^{\frac{1}{2}}} \times \exp\left(-\left\{ \frac{Aq}{(\pi)^{\frac{1}{2}}} \left[1 - \frac{A^2 Z}{\pi} \right]^{\frac{1}{2}} (\theta - \theta_B) + \frac{Ah}{\pi} \left[1 - \frac{A^2 Z}{\pi} \right]^{\frac{1}{2}} \right\}^2 \right), \tag{18}$$

where

$$q = \pi\, t_0\, \gamma_0 \sin 2\theta_B / A\lambda, \quad Z = q^2 \Big/ \left(\frac{1}{2\eta^2} + \frac{q^2 A^2}{\pi} \right),$$

$$h = (1 - \gamma_0/\gamma_H)/2F[\gamma_0/\gamma_H]^{\frac{1}{2}},$$

and where the half-width of the diffracted beam from a mosaic block is $(\pi \ln 2)^{\frac{1}{2}}/qA$. The integrated reflecting power for nonabsorbing crystals (i.e., $\sigma \gg \mu$, where μ = absorption per unit thickness) is

$$\mathcal{R}_\theta = \int_{-\infty}^{+\infty} \frac{\sigma T}{1 + \sigma T} d\theta. \tag{19}$$

This integral has been evaluated numerically and yields

$$\mathcal{R}_\theta = \frac{\pi^{\frac{1}{2}} f(s)}{Aq[1 - \pi^{-1} A^2 Z]^{\frac{1}{2}}} = \frac{N\bar{\sigma}T}{\gamma_0} \ll 1, \tag{20}$$

where $f(s)$ is plotted in Fig. 2 and where $s = (\sigma T)_{\theta = \theta_B}$.

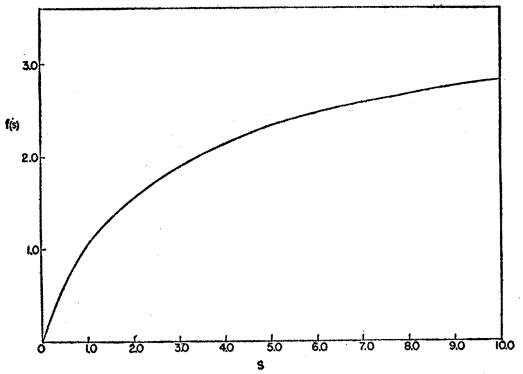

FIG. 2. Extinction factor $f(s)$ for the integrated reflecting power of an imperfect crystal as a function of s, $[s = (\sigma T)_{\theta = \theta_B}]$.

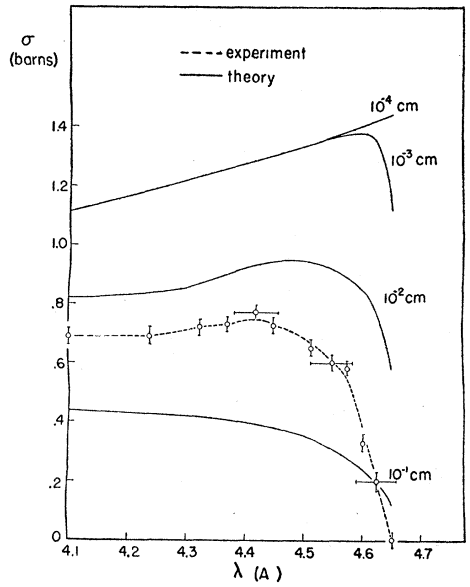

FIG. 3. Total cross section in barns of 111 peak in $\sim 2\times 10^{-2}$ cm polycrystalline aluminum as a function of neutron wavelength. with capture and inelastic scattering subtracted. Included are theoretical curves for varying gram sizes using 1.5 barn for σ_{COH}.

The general expression for the cross section is, including all factors,

$$\bar{\sigma}=\sum_{\lambda\leq 2d}\frac{\gamma_0\pi^{\frac{1}{2}}f(s)je^{-2w}\cos\theta_B}{2NAqT[1-\pi^{-1}A^2Z]^{\frac{1}{2}}}. \tag{21}$$

For $\sigma T\ll 1$, $f(s)=\pi^{\frac{1}{2}}(\sigma T)_{\theta=\theta_B}$ and the cross section reduces to (11). The condition for negligible secondary extinction (less than 5 percent) is $T\leq 0.05/\sigma_{\theta=\theta_B}$, where σ is given by (18).

When $\theta_B\to\pi/2$ for the last peak and for large σT, $f(s)\to\sim 3$ and $A^2q^2/\pi\ll 1/2\eta^2$. We then have

$$\bar{\sigma}\cong\frac{3dje^{-2w}}{2\pi^{\frac{1}{2}}t_0NT}. \tag{22}$$

In this case $\bar{\sigma}$ is independent of λ. Likewise, for σT large but $\theta_B<\pi/2$, $A^2q^2/\pi\gg 1/2\eta^2$ and

$$\bar{\sigma}\cong\frac{3\sqrt{2}\eta\cos\theta_Bje^{-2w}}{\pi NT}. \tag{23}$$

In this case $\bar{\sigma}$ decreases with λ.

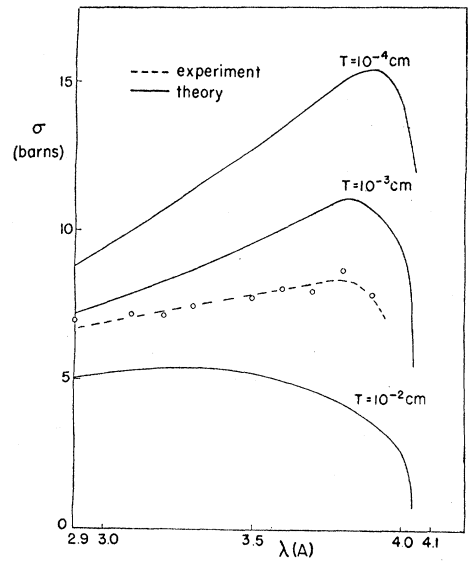

FIG. 4. Total cross section of 110 peak in Armco iron of grain size $\sim 7\times 10^{-3}$ cm as a function of neutron wavelength, with capture, incoherent, and inelastic scattering subtracted. Included are theoretical curves for varying grain sizes using 11.4 barn for σ_{COH}.

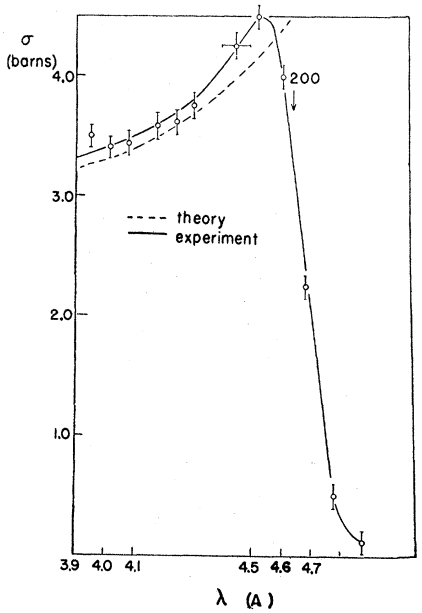

FIG. 5. Total cross section of 200 peak in very finely powdered NaF with capture, incoherent, inelastic and a small 111 scattering contribution subtracted. Included is a theoretical curve assuming no extinction, and using 1.5 barn for σ_{COH} of Na and 3.8 barn for σ_{COH} of F.

By observing the cross section for large σT far (23) and very close (22) to the cutoff we can experimentally determine η and t_0. The comments of the last two paragraphs under Primary Extinction are also applicable in the case of secondary extinction.

COMPARISON WITH EXPERIMENT

Figure 3 is a curve for polycrystalline 2*S* aluminum taken with a spectrometer at Brookhaven consisting of a lead crystal for selecting monochromatic neutrons, plus a beryllium filter to eliminate higher orders. This method gives good resolution and high intensity from 3.6A to 5.7A. Included in Fig. 3 are the theoretical curves for varying grain sizes (assuming $\eta=10^{-3}$), and they indicate the approach to extinction. It is quite

evident that primary extinction is not taking place, since application of Eq. (17) in the range 4.3 to 4.65A, where $\Delta\epsilon > \eta$, yields a cross section $\bar{\sigma}=0.06$ barn. The grain size of the aluminum is $\sim 2\times 10^{-2}$ cm. By increasing η to 2×10^{-3} cm better agreement is obtained.

Figure 4 is a similar curve for Armco iron of $\sim 7\times 10^{-3}$ cm grain size, taken by Hughes *et al.* at the Argonne National Laboratory.[7] The presence of extinction is quite apparent. Figure 5 is a curve (taken with the lead crystal) of very finely powdered NaF, together with a theoretical curve calculated from (11). We find good agreement with the theory for negligible extinction.

The determination of the mosaic block size from Eq. (22) requires better resolution than was obtained by the spectrometer used above. A resolution, $\Delta\lambda/\lambda$, of approximately 0.005 is required, whereas we have a resolution of 0.02. Such resolution is feasible and is planned for a future project.

We wish to express our thanks to D. J. Hughes, S. Pasternack, A. W. McReynolds, L. D. Jaffé, J. C. Slater, D. Kleinman, L. Corliss, and J. Hastings for many interesting discussions and suggestions.

[7] Hughes, Wallace, and Holtzman, Phys. Rev. **73**, 1277 (1948).

PHYSICAL REVIEW VOLUME 86, NUMBER 3 MAY 1, 1952

Evidence for K-Shell Ionization Accompanying the Alpha-Decay of Po^{210}

W. C. BARBER* AND R. H. HELM
Department of Physics, Stanford University, Stanford, California
(Received October 8, 1951)

The radiations of Po^{210} have been studied using NaI scintillation counters. In agreement with Grace, Allen, West, and Halban, it is concluded that the soft electromagnetic component probably entirely consists of x-rays of lead. The region from 25 kev to 2.5 Mev has been examined and, with the exception of the known γ-ray of 800 kev, no nuclear γ-rays were observed. The ratio of the number of K x-rays to the number of 800-kev γ-rays was measured as 0.134 ± 0.025 to 1. The K shell internal conversion coefficient of the 800-kev transition has been reported as about 0.05, and hence the K x-ray intensity is too great to be explained by internal conversion alone. The residual x-rays are attributed to the process whereby the emission of the alpha-particle causes ionization of the atom. Comparison of the relative intensity of K x-rays and alpha-particles shows qualitative agreement with the probability of this ionization process as calculated by Migdal.

I. INTRODUCTION

ZAJAC, Broda, and Feather[1] have reported γ-rays of energy 84 ± 4 kev in the decay of 138-day Po^{210}. In investigating Po^{210} radiations with NaI scintillation counters we have observed radiation in this energy region, but our measurements yield a mean energy of 76 kev. In attempting to understand the origin of this radiation we have measured its intensity relative to the intensity of the 800-kev γ-ray, and we have looked for coincidences between the 800- and the 76-kev radiations. The results of our investigations are consistent with the interpretation of the softer radiation as x-rays of lead, whereas its interpretation as a nuclear γ-ray would lead to an unlikely decay scheme. The energy resolution of our counters is not sufficient to resolve the K_α and K_β x-rays of lead, and hence we would not be able to distinguish a 76-kev nuclear γ-ray from the lead K x-ray spectrum. However, during the time our measurements were being made, Grace, Allen, West, and Halban[2] reported the result of an investigation of the Po^{210} spectrum where the soft radiations were detected in proportional counters. In their work lines interpretable as the K_α and K_β were observed, and with the help of critical absorption measurements they were determined to be x-rays of lead. Grace *et al.*[2] measured the number of K x-rays relative to alpha-particles and also the number of conversion electrons relative to alpha-particles. Noting that these were experimentally equal they explained the x-rays as the result of the internal conversion of the 800-kev γ-ray.

Our results for the most part are in agreement with the work of Grace *et al.*,[2] but on the question of the relative intensity of K x-rays and conversion electrons we find evidence for more quanta than can be accounted for by internal conversion alone. Since this is the most important contribution of the present paper, we should like to note, as will be shown in the concluding section, that when the data of Grace *et al.*[2] are corrected for the Auger effect and the K/L internal conversion ratio they are not in disagreement with our conclusion.

II. EXPERIMENTAL METHODS

The polonium was supplied by the Eldorado Mining and Refining Company, who report radioactive impurities (of unspecified form) of about 6×10^{-6} mg of Ra-equivalent per millicurie of Po. The sources were prepared for use and further purified by precipitation

* Now at Microwave Laboratory, Stanford University, Stanford, California.
[1] Zajac, Broda, and Feather, Proc. Phys. Soc. (London) **60**, 501 (1948).
[2] Grace, Allen, West, and Halban, Proc. Phys. Soc. (London) **64**, 493 (1951).